

AD-A018 805

**BOUNDARY LAYER TRANSITION ON BLUNT BODIES IN  
HYPERSONIC FLOW**

**B. E. Richards**

**Von Karman Institute for Fluid Dynamics**

**Prepared for:**

**Air Force Materials Laboratory  
European Office of Aerospace Research and Development**

**September 1975**

**DISTRIBUTED BY:**

**NTIS**

**National Technical Information Service  
U. S. DEPARTMENT OF COMMERCE**

006067

AFML-TR-75-139

ADA018805

# BOUNDARY LAYER TRANSITION ON BLUNT BODIES IN HYPERSONIC FLOW

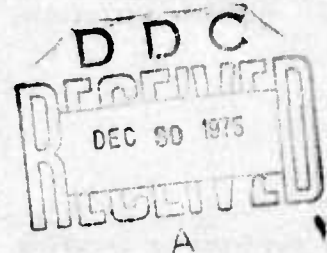
VON KARMAN INSTITUTE FOR FLUID DYNAMICS  
CHAUSSÉE DE WATERLOO, 72  
1640 RHODE-ST-GENÈSE, BELGIUM

SEPTEMBER 1975

TECHNICAL REPORT AFML-TR-75-139  
INTERIM SCIENTIFIC REPORT DECEMBER 1973 - MAY 1974

Approved for public release; distribution unlimited

Reproduced by  
NATIONAL TECHNICAL  
INFORMATION SERVICE  
U.S. Department of Commerce  
Springfield, VA. 22151



AIR FORCE MATERIALS LABORATORY  
AIR FORCE WRIGHT AERONAUTICAL LABORATORIES  
Air Force Systems Command  
Wright-Patterson Air Force Base, Ohio 45433





Unclassified

SECURITY CLASSIFICATION OF THIS PAGE(When Data Entered)

well with reference enthalpy prediction methods except for 0.004 inch mean element height wall roughness generated turbulent boundary layer cases when 35 per cent higher values than theory were measured. Transition occurred on the  $50^\circ$  half angle cone forebody in the region of  $270 < Re < 400$  or  $10^5 < Re_s < 2.5 \times 10^5$  for smooth surfaced models and  $170 < Re_s < 300$  and  $4 \times 10^4 < Re_s < 10^5$  for rough surfaced models. The Reynolds number range of the roughness height  $k$  on the rough models was  $83 < Re_k < 500$ .

Unclassified

SECURITY CLASSIFICATION OF THIS PAGE(When Data Entered)

## PREFACE

The activities and results documented in this report were supported under project 7381 "Materials Application," Task 7381-02 "Space, Missile and Propulsion System Materials and Component evaluation" with Mr. Gary L. Denman, Technical Manager for Thermal Protective Systems, System Support Division, Air Force Materials Laboratory, acting as project engineer. The report covers work carried out during the period December 1973 to May 1974.

The technical advice and guidance by Mr. Victor Di Cristina, Manager, Thermodynamics and Material Test Department, Avco Systems Division, Avco Corporation, Wilmington, in the areas of model design and instrumentation and suggested test series were particularly valuable. The author wishes to express his gratitude for the assistance given by Mr. Michael A. Kenworthy and Mr. Cyriel Appels, Research Assistants in the Aeronautics/Aerospace Department in the data reduction of the tests, and Mr. Jean Hugé and members of the Longshot personnel in carrying out the tests.

## TABLE OF CONTENTS

SECTION	PAGE
I. INTRODUCTION	1
II. EXPERIMENTAL PROCEDURE	5
1. Models and their instrumentation	5
2. Test Facility	8
III. RESULTS AND DISCUSSION	13
1. Schlieren studies	13
2. Pressure measurements	13
n    3. Heat transfer measurements	16
4. Transition detection results	26
IV. CONCLUSIONS	33
REFERENCES	34

## LIST OF FIGURES

FIGURE	PAGE
1. Schematic of Biconic Models.	6
2. Photographs of Models A and G.	7
3. Typical Schlieren Photographs of the Flow Over Models A and G.	7
4. Pressure Distributions on Biconic Model Forebody.	15
5. Heat Transfer Distribution on Model G at $M=15.5$ and $Re/ft = 4.6 \times 10^6$ (Run 376).	18
6. Heat Transfer Distribution on Model G at $M=19.2$ and $Re/ft = 2.1 \times 10^6$ (Run 377)	19
7. Heat Transfer Distribution on Model A at $M=15.5$ and $Re/ft = 4.6 \times 10^6$ (Run 378)	20
8. Heat Transfer Distribution on Model F at $M=19.2$ and $Re/ft = 2.1 \times 10^6$ (Run 379)	21
9. Heat Transfer Distribution on Model C at $M=16.0$ and $Re/ft = 8.7 \times 10^6$ (Run 380)	22
10. Heat Transfer Distribution on Model A at $M=19.2$ and $Re/ft = 2.1 \times 10^6$ (Run 354)	23
11. Heat Transfer Distribution on Model A at $M=16.0$ and $Re/ft = 8.7 \times 10^6$ (Run 356)	24
12. Heat Transfer Distribution on Model F at $M=16.0$ and $Re/ft = 8.7 \times 10^6$ (Run 351)	25
13. Estimation of Location of Boundary Layer Flow Regimes in $Re_{\theta}$ and $Re_s$ . Smooth Models.	29
14. Estimation of Location of Boundary Layer Flow Regimes in $Be_{\theta}$ and $Re_s$ . Rough Models.	30



## LIST OF TABLES

1. Heat Transfer Sensor Calibration Constants (Btu/ft<sup>2</sup>sec)/  
(mv/sec) .
2. Typical Longshot Test Section Conditions.
3. Estimated Test Section Conditions at Model Nose-tip  
at Time T = 0 msecs from Peak.
4. Pressure Measurement at Time T = 0 msecs (lb/in<sup>2</sup>)
5. Heat Transfer Measurement at Time T = 0 msecs  
(Btu/ft<sup>2</sup>sec).
6. Position of Transition ,s<sub>t</sub>, on 50° Half Angle Biconic  
Model Forebody.

## SECTION I

### INTRODUCTION

Knowledge of the position of boundary layer transition on surfaces at large angles to a high speed flow is of vital importance in the design of re-entry vehicle heat protection systems. Two current design applications are the following. The NASA Space Shuttle is planned to re-enter the atmosphere at the high angles of attack required to achieve maximum  $C_L$ . This manoeuvre is used to keep heating rates low by allowing deceleration to occur in the less dense atmospheres present at high altitudes. The prediction of the position of transition on the high incidence undersurfaces of the vehicle will affect the selection of the re-usable thermal protection systems planned. In design of ablation nose tips of re-entry vehicles, local heat transfer rates in the stagnation region, and hence local surface shape and nose recession rates are expected to be drastically changed by the location of boundary layer transition.

So far prediction of transition using analytical means has defied scientists, ( see for example Ref. 1 ) and hence correlations of existing data are generally used. The main problem of transition prediction is that many parameters affect the phenomenon (e.g. Mach number, unit Reynolds number, wall temperatures, pressure gradient, free stream disturbances, wall roughness, flow history) and difficulty is found in isolating their respective effects on transition location.

One, strongly pursued analytical method of predicting trends of transition behaviour is by employing the assumption that the transition point occurs at a certain level of

amplification of two dimensional disturbances after the critical Reynolds number of stability is achieved. Typical calculations of the stability of the compressible laminar boundary layer are given by Mack (Ref. 2) and an appropriate transition criterion is that given by Smith and Gamberoni (Ref. 3).

The main uncertainty of this approach is associated with the early change of the flow behaviour in the transition region from that assumed in parallel flow stability to a strongly non-linear three dimensional flow which is difficult to predict analytically (Ref. 4). However, the NASA Transition Study Group is carrying out extensive fundamental studies to prove the efficacy of this approach (Ref. 5). One of their chief concerns is the verification of the usefulness of wind tunnel generated data, providing an uncertainty due to disturbances in the test environment. Generalised correlations of data have met with no more success (Ref. 1), and many anomalies still exist. Examples are: the unexpected existence of unit Reynolds number effects; trend reversals due to wall cooling and the very low transition Reynolds numbers met on blunt bodies, detected and of relevance to this present study. These findings indicate that great caution has to be taken when applying general correlations of data and since this empirical approach has to be used by designers before the phenomena is more better understood, that correlations with more limited ranges of applications should be generated and applied.

The most used non-dimensional parameter to define the location of transition in these empirical approaches is the Reynolds number based on the distance from the flow stagnation point to a stated position in the transition region (e.g. beginning, mid-point, end as defined by the

measurement used to locate transition). This parameter is inappropriate to apply to correlations associated with vehicle shapes with blunt bodies since it is usually difficult to define the stagnation point, and furthermore the boundary layer has often developed in changing flow conditions. Another parameter which is frequently used for correlations is a Reynolds number based on local flow conditions and a length scaled on a local characteristic boundary layer thickness, assumed to have grown lamina rly up to that point. The momentum thickness,  $\theta$ , is often selected since this is usually known from the integral boundary layer solutions required to calculate the skin friction over complicated shapes. Another parameter is the displacement thickness  $\delta^*$  often known on vehicles in high Mach number flows where boundary layer interaction is important. For application to the present study of transition over surfaces at high angles to high speed flow then the Reynolds number based on the momentum thickness,  $Re_\theta$ , is considered to be the most appropriate.

Data generated in the low Mach number high static temperature flows typical of that obtained over blunt bodies in high speed flow have shown the striking feature that transition occurs at a very low Reynolds number. This is unexpected since the boundary layers are developing under cold wall and also often under favourable pressure gradient conditions, two cases for which boundary layer stability theory would indicate the existence of prolonged regions of lamina r boundary layers. It is this unexpected feature that led to studies of heat-sink type protection systems, considered earlier from such stability theory considerations to have optimum design features, to be rejected (Ref. 6). Transition occurred at Reynolds numbers sometimes even

below the critical Reynolds numbers. This and other anomalous transitional behaviour has led Morkovin (Ref. 1) to consider that there are several different paths leading from laminar to turbulent flows.

Transition data in the conditions of interest have rarely been published in the literature. Facilities with the capability to generate low Mach number at high static temperatures are selectively few. Some data has been generated in free flight experiments, such as described by Murphy and Rubesin (Ref. 6) however difficulties lie in defining the conditions under which the experiments were carried out. Shock tube flows also are capable of generating representative conditions (e.g. as in tests described by Hartunian et al, (Ref. 7) however some difficulty lies in interpreting the results from the unsteady boundary layers thus generated. Recent tests in the VKI Longshot facility, specifically designed for simulating re-entry flows (Ref.8) , have shown that laminar, transitional and turbulent flows can be generated on surfaces at high angles of attack (Ref. 9) in which typically the local Mach number is 1.5 at static temperatures of over 2400°K.

The present series of tests were planned to examine the behaviour of the transition point on blunt body shapes under changing conditions of Mach numbers Reynolds number, surface roughness and model shape. Comparisons with simple correlation methods of these results, and those from earlier tests in this series (Ref. 9, 10), are made with a view to applying such correlations to the results of a larger program on heat transfer over ablation nose-shapes ongoing at VKI.

## SECTION II

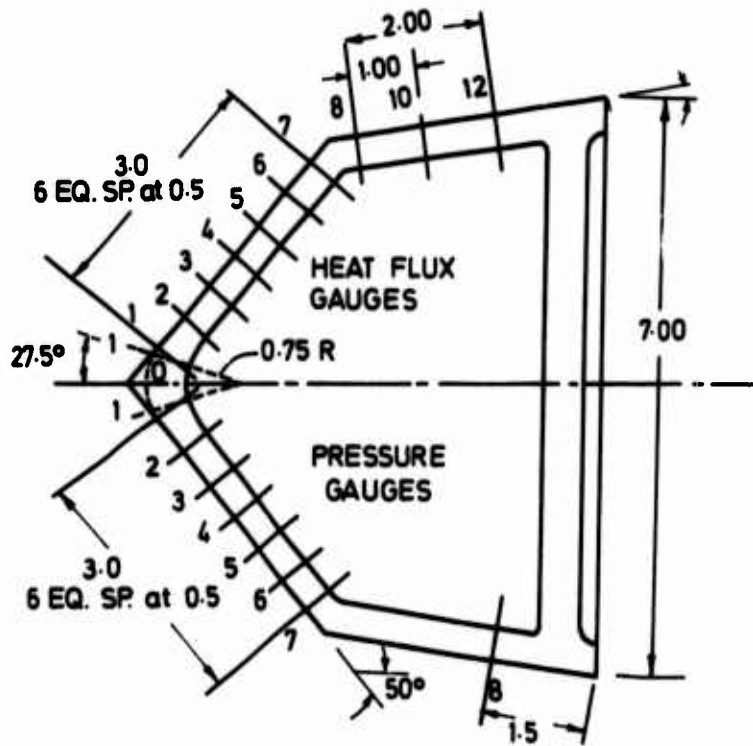
### EXPERIMENTAL PROCEDURE

#### 1. MODELS AND THEIR INSTRUMENTATION.

Two steel biconic models, supplied by Avco, with  $50^\circ$  half angle forebodies,  $8^\circ$  half angle after bodies and 7 in base diameter as sketched in Fig 1 were used in this test series. One model had a smooth surface, the other had the forebody surface uniformly roughened using a metal spraying technique to a mean height of 0.004 in. Each model could be fitted with either a pointed nose or a spherical nose with 0.75 in radius. The smooth surfaced models are designated model A and C for the sharp and blunt configurations. The equivalent designation for the rough model configurations are F and G. A photograph of models A and G is shown in Fig. 2. A sharp nosed model with 0.040 in machined roughness on the forebody and used in earlier tests (Ref. 10) is also referred to in the test. It is designated Model B.

Nine (or ten in the case of the blunt configurations) heat transfer gauges were mounted axially along and flush with the model surface beginning at or near the geometric stagnation point as shown in Fig. 1. Eight pressure taps were similarly spaced along the surface but at  $180^\circ$  around the model from the heat transfer gauges.

Pressures were measured using Hidyne variable reluctance pressure transducers. Their description, mounting and calibration is described in Ref.10. The heat sensors consist of 0.125 in diameter copper discs bonded to insulated holders. Chromel-Alumel thermocouples with diameters of 0.001 in. were welded to the backface of the discs. The heat sensors mounted in the rough models usually differed from those mounted on the smooth models by the



Dimensions in inches

FIG. 1 SCHEMATIC OF BICONIC MODELS

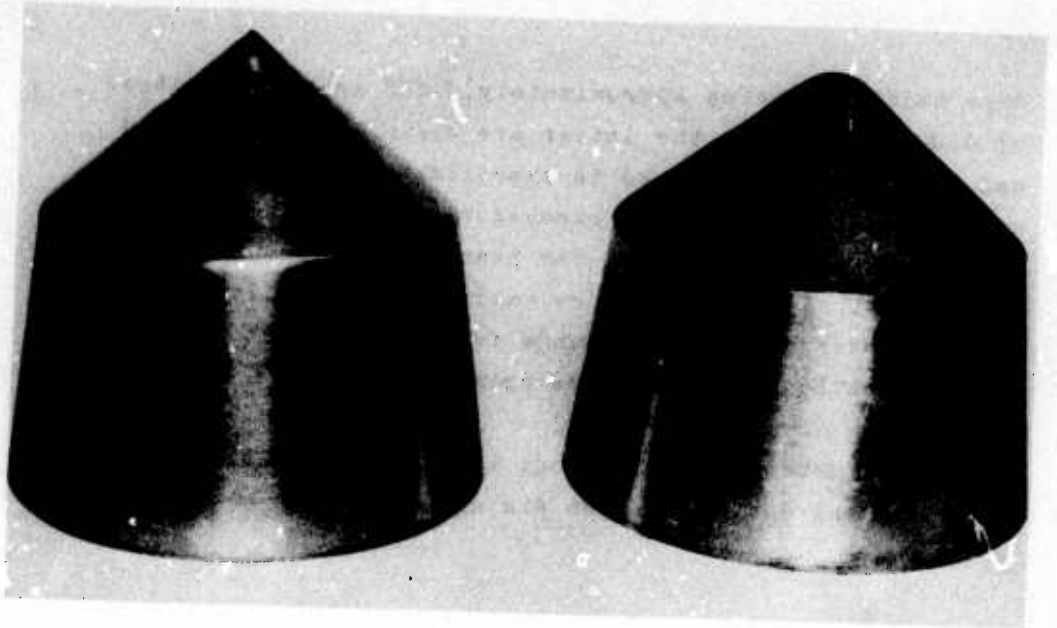


**FIG. 2 PHOTOGRAPH OF MODELS A and G**

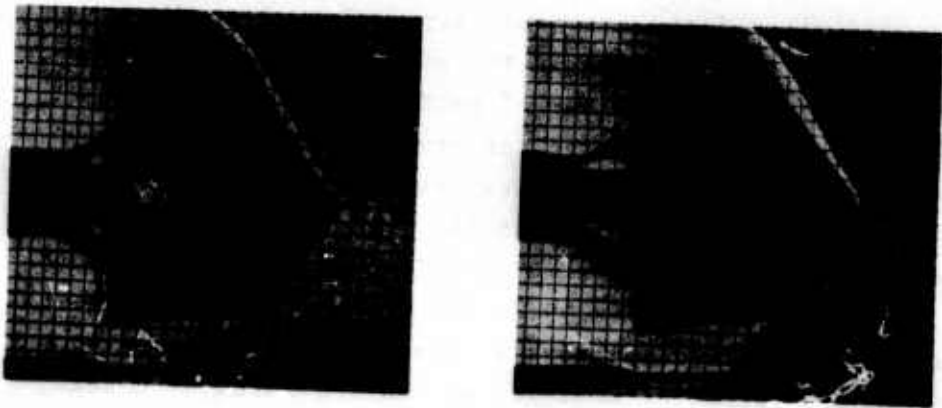


**FIG. 3 TYPICAL SCHLIEREN PHOTOGRAPHS OF THE FLOW OVER MODELS A and G**



disc thickness being approximately 0.008 in. thick instead of 0.004 in. thick ( the latter are described in Ref. 10 ) and furthermore roughened to approximately the same extent as the model surface. The exposed surface of the insulating holder was also roughened. The heat gauges were calibrated in the AEDC radiant heat flow calibration facility before mounting over a heat flux range from 20 to 80 Btu/ft<sup>2</sup>sec. The calibration constants are presented in Table 1 .

Further details about the instrumentation, signal recording and data reduction are given in Ref. 10 .

## 2. TEST FACILITY

The VKI Longshot facility was used exclusively for this program. Longshot differs from a conventional gun tunnel in that a heavy piston is used to compress the nitrogen test gas to very high pressure and temperatures (Ref. 8). The test gas is then trapped in a reservoir at peak conditions by the closing of a system of check valves. The flow conditions decay monotonically during 10 to 20 milliseconds running time as the nitrogen trapped in the reservoir flows through the 6° half angle conical nozzle into the pre-evacuated open jet test chamber. The maximum supply conditions used in these tests are approximately 60,000 lb/in<sup>2</sup> at 1900°K to 2350°K. These provide unit Reynolds numbers of  $8.5 \times 10^6$  per foot at a Mach number of 16 and  $3 \times 10^6$  at  $M = 19.8$ . Table 2 lists the four most used test section conditions at the nozzle exit achieved at the peak operation achieved at the beginning of a test. These values are slightly revised from previous values published due to an exhaustive revision of the interpretation

TABLE I

HEAT TRANSFER SENSOR CALIBRATION CONSTANTS  
(BTU/FT<sup>2</sup>) / (MU/SEC)

MODEL	A	C	F	G
Gauge N° 0	-	0.818*	-	0.929
1	0.818*	0.818*	1.911	1.911
2	0.890	0.890	1.796	1.796
3	0.830	0.830	1.857	1.857
4	0.818*	0.818*	4.012	4.012
5	0.740	0.740	1.826	1.826
6	0.818*	0.818*	1.747	1.747
7	0.730	0.730	1.950	1.950
8	0.810	0.810	1.836	1.836
9	-	-	1.778	1.778
10	0.818*	0.818	2.196	2.196
12	0.910	0.910	-	-

\* uncalibrated gauges, average value of 0.818 for Models A and C used.

TABLE 2

TYPICAL LONGSHOT TEST SECTION CONDITIONS

	T(MS)	PO(PS1)	TO(K)	P1TOT(PSI)
	MACH NO	POP(PS1)	TO P(K)	RE/FT
	P(PS1)	T(K)	RHO	V(FT/SEC)
	QD(LB/FT**2)	Q(BTU)	TT2R(K)	CONDENSATION
1.	0.000	0.550000E 05	0.190000E 04	0.200000E 02
	15.990	0.798927E 05	0.245702E 04	0.872964E 07
	0.780727E-01	0.471264E 02	0.746250E-04	0.734354E 04
	0.201217E 04	0.939885E 02	0.219290E 04	0.432018E 02
2.	0.000	0.350000E 05	0.202000E 04	0.150999E 02
	15.470	0.394981E 05	0.247216E 04	0.465051E 07
	0.484203E-01	0.505899E 02	0.431134E-04	0.736132E 04
	0.116814E 04	0.721548E 02	0.220516E 04	0.408538E 02
3.	0.000	0.590000E 05	0.235000E 04	0.800000E 01
	19.906	0.716570E 05	0.303464E 04	0.313777E 07
	0.154730E-01	0.378117E 02	0.184330E-04	0.818913E 04
	0.618078E 03	0.668823E 02	0.265925E 04	0.368548E 02
4.	0.000	0.376000E 05	0.232000E 04	0.519999E 01
	19.178	0.388046E 05	0.286190E 04	0.206365E 07
	0.108387E-01	0.383805E 02	0.127209E-04	0.794881E 04
	0.401877E 03	0.503513E 02	0.252000E 04	0.354101E 02

Case 1,  $M_{nom} = 15$ , High Re.

Case 2,  $M_{nom} = 15$ , Low Re.

Case 3,  $M_{nom} = 20$ , High Re.

Case 4,  $M_{nom} = 20$ , Low Re.

See text for nomenclature.

of the reservoir temperature measurements as described in a report by Backx (Ref. 11). The following nomenclature is used in Table 2 : measured reservoir pressure  $P_0$  (psi); measured reservoir temperature,  $T_0$  ( $^{\circ}K$ ); measured Pitot pressure,  $PITOT$  (psi); calculated Mach number ,  $MACH$  NO; equivalent perfect pressure,  $POP$  (psi); equivalent perfect temperature,  $TOP$  ( $^{\circ}K$ ); freestream Reynolds number per ft;  $RE/FT$ ; local freestream pressure  $P$ , (psi); freestream temperature,  $T$  ( $^{\circ}K$ ); freestream density,  $RHO$  (slugs/ft<sup>3</sup>); stream velocity,  $V$ (ft/sec); dynamic pressure,  $QD$  (lb/ft<sup>2</sup>); stagnation point heating on a 7 in diameter spherical surface,  $Q$  (Btu/ft<sup>2</sup>sec); true stagnation temperature,  $TT2R$  ( $^{\circ}K$ ); and the temperature at which condensation would occur at that freestream pressure and expansion rate,  $CONDENSATION$  ( $^{\circ}K$ ). These parameters adequately define all the parameters necessary for application to predictive procedures. Care should be taken in that the accuracy of the values printed out should not be inferred from the six significant figures shown. The accuracy is controlled by the accuracy of the measurements inferred in Ref. 10.

Reservoir pressures and temperatures were measured with Kistler quartz piezo-electric sensors and tungsten-rhenium thermocouples, respectively. Flow visualisation photographs were taken with an 18 in diameter Toepler schlieren system using a 1  $\mu$  sec duration spark to illuminate the flow.

The test matrix covered in this test series is outlined in Table 3 .Other tests from earlier phases (Refs. 9 and 10) have also been referred to in the discussion given later.

TABLE 3

ESTIMATED TEST CONDITIONS AT NOSE OF MODELS AT TIME  $T = 0$  msec FROM PEAK

RUN	MODEL	AVCO RUN No	$P_0$	$T_0$	Pitot	$M$	$Re \times 10^{-6}$	$q_D$	$q$
376	G	4	35,000	2020	15.1	15.5	4.6	1168	72.1
377	G	5	37,600	2320	5.2	19.2	2.1	402	50.3
378	A	1	35,000	2020	15.1	15.5	4.6	1168	72.1
379	F	3	37,600	2320	5.2	19.2	2.1	402	50.3
380	C	2	55,000	1900	26.0	16.0	8.7	2010	94.0

Units .  $P_0$  and pitot (lb/in<sup>2</sup>); dynamic pressure,  $q_D$  (lb/ft<sup>2</sup>);  
 $T_0$  (°K);  $Re$  (ft<sup>-1</sup>); stagnation point heat transfer,  $q$ ,  
 BTU/ft<sup>2</sup> sec.

Details of other runs referred to are given in Ref. 9 and 10. Since these letter reports, interpretation of the reservoir temperature thermocouple outputs has been re-assessed as in Ref. 11. Table 2 can be referred to, to up date these earlier results.

↖ conditions at exit plane of nozzle.

## SECTION III

### RESULTS AND DISCUSSION.

#### 1. SCHLIEREN STUDIES.

Typical schlieren photographs from the series are shown in Fig. 3. Although the shock wave structure is shown very clearly in each photograph the boundary layer growth on the model is too small to be distinct. The schlieren method of detecting transition hence cannot be used. In some of the photographs, there are signs of waves in the shock layer which may be ascribed to the sound disturbances radiating from the turbulent boundary layer similar to that seen for example by Brinich (Ref. 12). This observation however is not clear enough to be able to provide a transition detection technique.

#### 2. PRESSURE MEASUREMENTS.

Measurements of the peak values of pressure are tabulated in Table 4 and their values, non-dimensionalised with respect to the dynamic pressure at the model nose, plotted in Fig. 4. General agreement with tangent cone theory is obtained, although considerable data scatter is found particularly in the rough surfaced model cases. This scatter is ascribed to the layer of roughness sprayed onto the model in some cases distorting the geometry around the pressure taps. Because this scatter is caused by disturbances local to the pressure tap, and that results on smooth bodies have shown excellent agreement with tangent cone theory with little scatter, it is advised that for predicting heat transfer rates using similarity theories, such as that of Lees (Ref. 13), the theoretical pressure variation be used.

TABLE 4

PRESSURE MEASUREMENTS at TIME T = 0 msec (lb/in<sup>2</sup>)

RUN N°	376	377	378	379	380
TEST CASE	M=15	M=20	M=15	M=20	M=15
MODEL	Low Re G	Low Re G	Low Re A	Low Re F	High Re C
Station 1	10.05	3.53	-	-	18.59
2	8.27	2.64	10.4	1.91	16.64
3	10.20	3.10	11.2	3.06	18.53
4	12.82	3.06	9.7	3.14	15.73
5	10.74	3.44	-	3.69	16.19
6	13.13	3.52	9.8	3.52	16.50
7	8.69	2.76	10.5	2.83	17.27
8	0.76	-	0.64	0.22	1.025

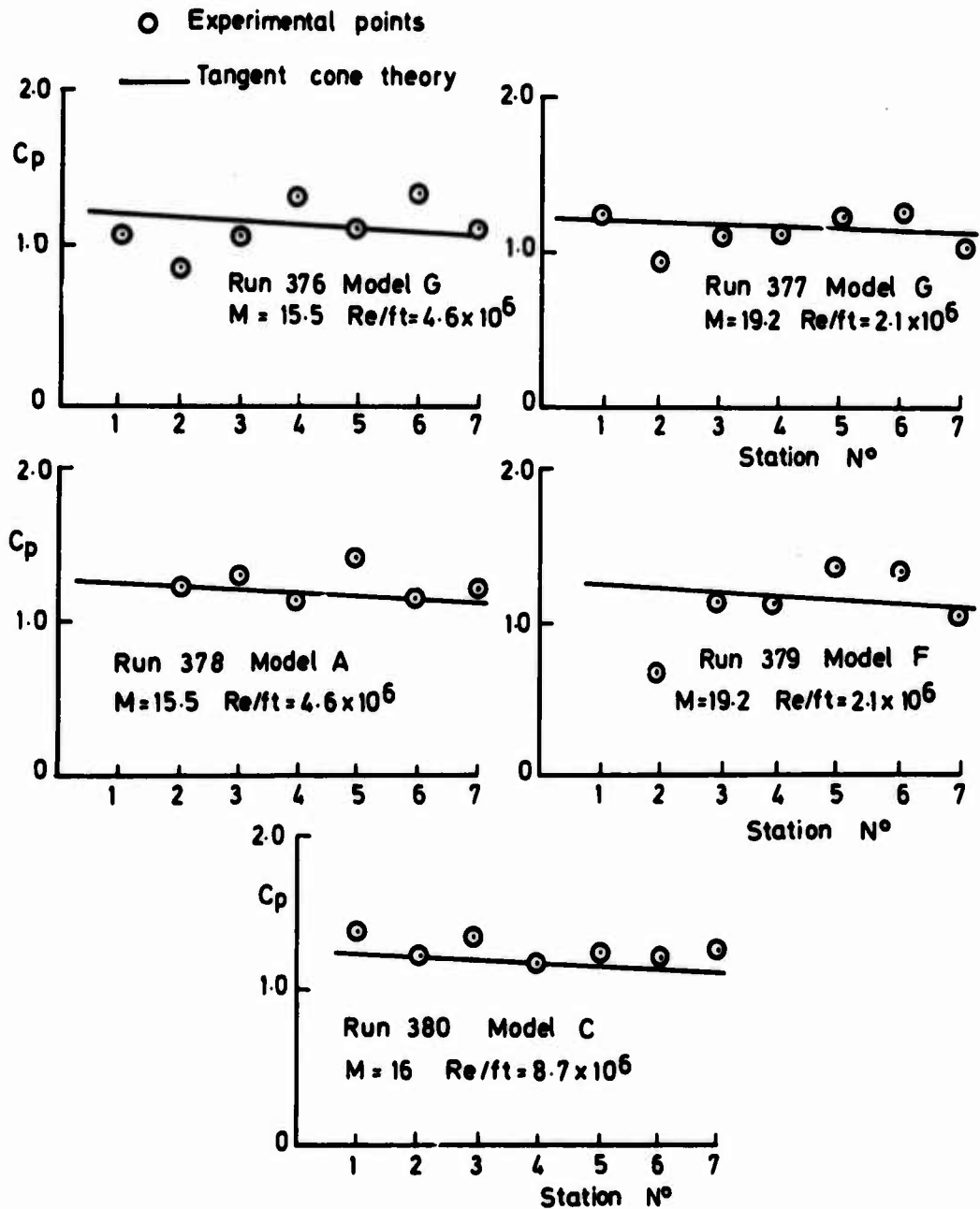


FIG 4 PRESSURE DISTRIBUTIONS ON BICONIC MODEL FOREBODY



### 3. HEAT TRANSFER MEASUREMENTS.

Measurements of the peak values of the heat transfer are tabulated in Table 5 and plotted in Figs. 5-9 against distance from the stagnation point,  $s$ . Also shown in the plots is the Reynolds number based on the distance from the nose,  $Re_s$ , and the Reynolds number based on the momentum thickness,  $Re_\theta$ , of a laminar boundary layer growing from the nose. These Reynolds numbers are calculated assuming the nose is pointed in all cases. The method of calculating  $Re_s$  is described in Appendix C of Ref. 10. The momentum thickness is calculated assuming a simple Blasius profile type approach.

The measurements are compared against the Eckert (Ref. 17) and Sommer - Short (Ref. 15) reference enthalpy methods found in earlier tests (Ref. 9) to predict wall laminar and turbulent heat transfer rates, respectively, on smooth bodies. Three sets of data (from run numbers 351, 355 and 356) obtained in this earlier test series are presented in Figs. 10 - 12 to illustrate this agreement and to show examples of fully laminar and fully turbulent flows not actually achieved in this test series. Another reason to illustrate these latter figures in this report is to compare the results with the theories modified from earlier test phases by making alterations to the assessed tunnel reservoir temperature as indicated by Backx (Ref. 11). These latter figures illustrate that the Eckert theory slightly underestimates laminar data and Sommer - Short theory agrees with smooth wall turbulent data but underestimates the rough wall data by 35 %. These conclusions are also generally to be found in the new data presented in Figs. 5-9 within the scatter of the results and the interpretation of

TABLE 5

HEAT TRANSFER MEASUREMENTS, TIME T = 0 msec (BTU/ft<sup>2</sup>sec)

RUN N°	376	377	378	379	380
TEST CASE	M=15.5	M=19.2	M=15.5	M=19.2	M=16
	Low Re	Low Re	Low Re	Low Re	High Re
MODEL	G	G	A	F	C
0	197	126	-	-	238
1	160	74	201	101	190
2	166	60	117	66	161
3	154	51	113	47	163
4	100 <sup>†</sup>	39 <sup>†</sup>	36 <sup>*</sup>	30 <sup>†</sup>	51 <sup>*</sup>
5	170	51	152	48	202
6	173	51	129	52	179
7	158	48	4 <sup>*</sup>	50	12 <sup>*</sup>
8	8.2	5.0	13.2	5.3	13.2
9	-	-	-	4.7	-
10	5.1	4.3	-	4.6	-
12	-	-	7.5	-	8.8

\* Rejected data due to suspect gauges.

† Low value may be due to poor gauge (see its calibration constant in Table 1).

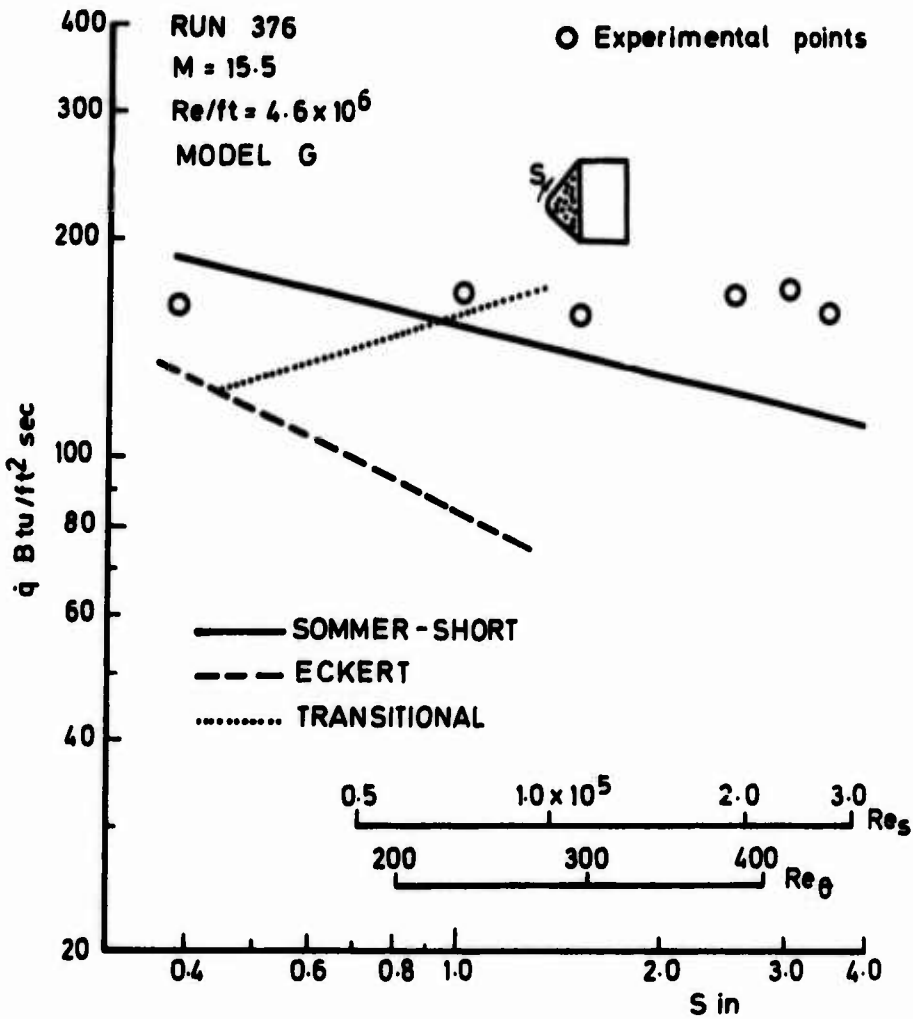


FIG. 5 HEAT TRANSFER DISTRIBUTION ON MODEL G  
AT  $M=15.5$   $RE/FT = 4.6 \times 10^6$

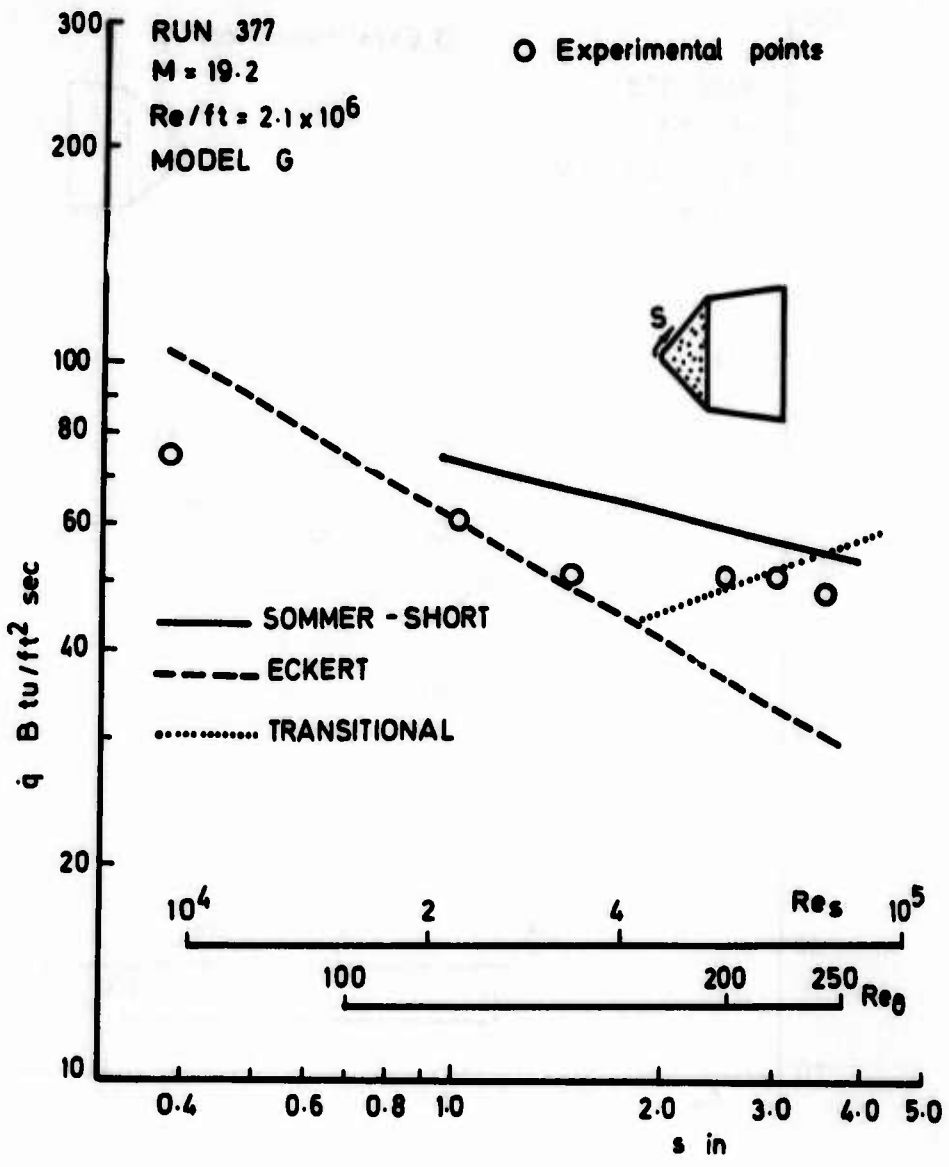


FIG. 6 HEAT TRANSFER DISTRIBUTION ON MODEL G  
 AT M = 19.2 RE / FT = 2.1 x 10<sup>6</sup>

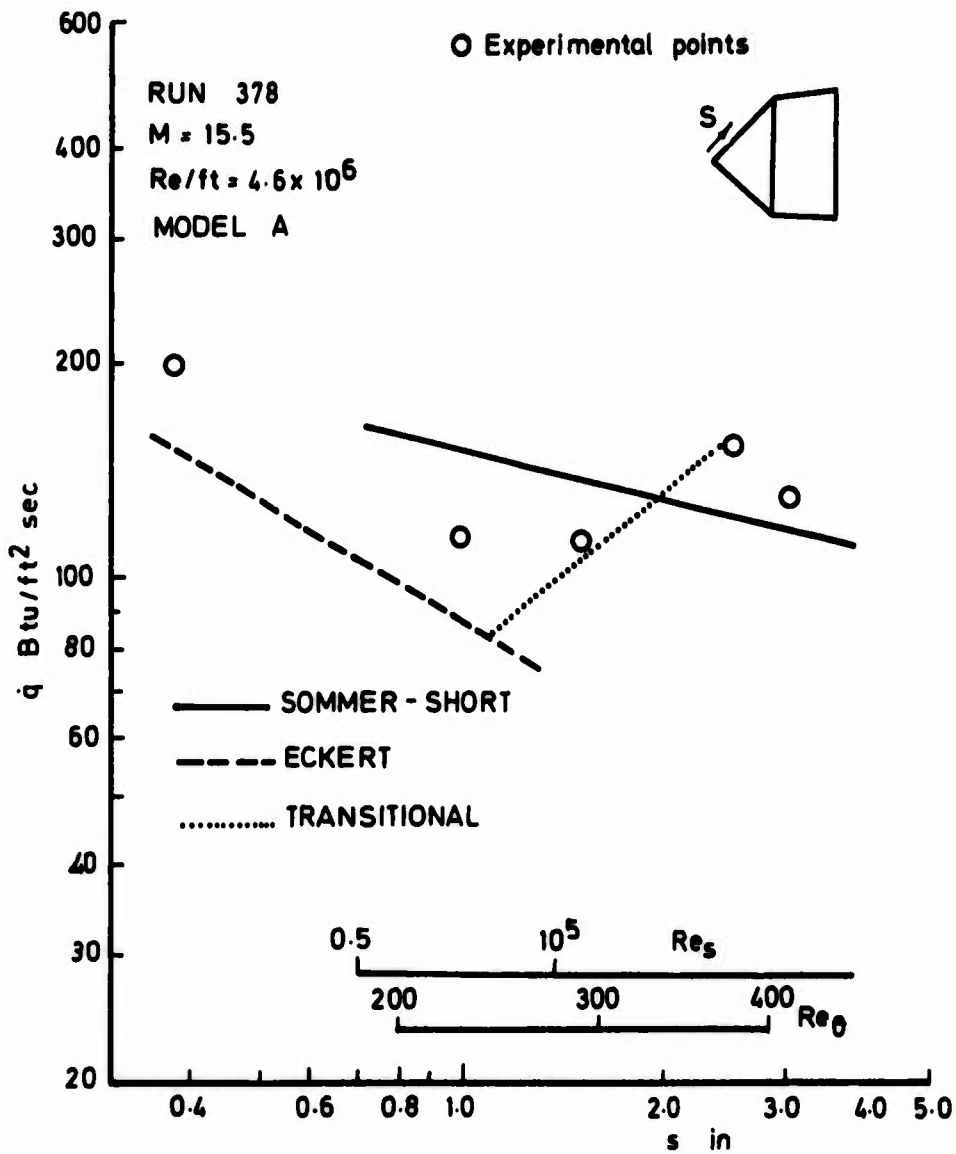


FIG. 7 HEAT TRANSFER DISTRIBUTION ON MODEL A  
 AT  $M = 15.5$   $RE/FT = 4.6 \times 10^6$

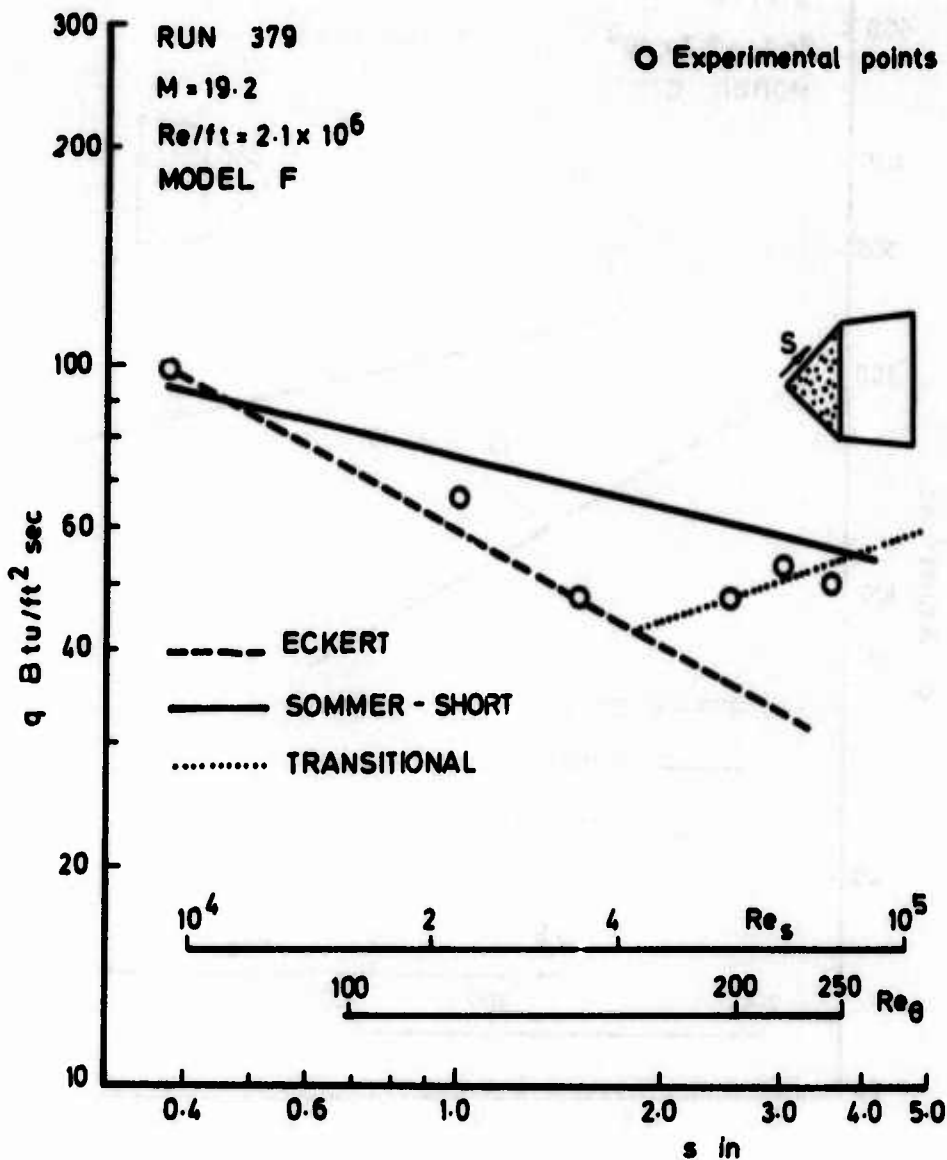


FIG. 8 HEAT TRANSFER DISTRIBUTION ON MODEL F  
 AT  $M = 19.2$   $RE/FT = 2.1 \times 10^6$

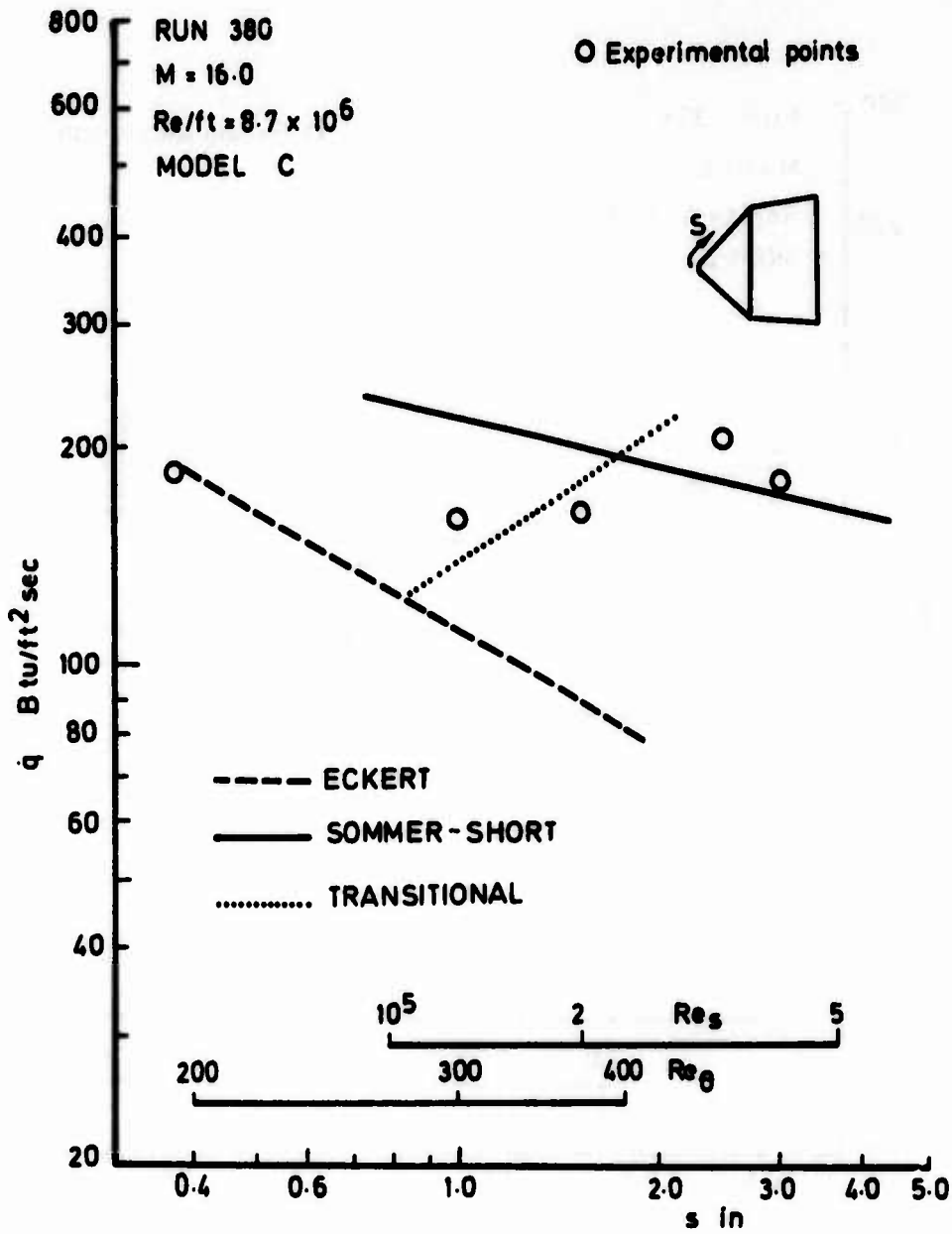


FIG. 9 HEAT TRANSFER DISTRIBUTION ON MODEL C  
 AT  $M = 16.0$   $RE / FT = 8.7 \times 10^6$

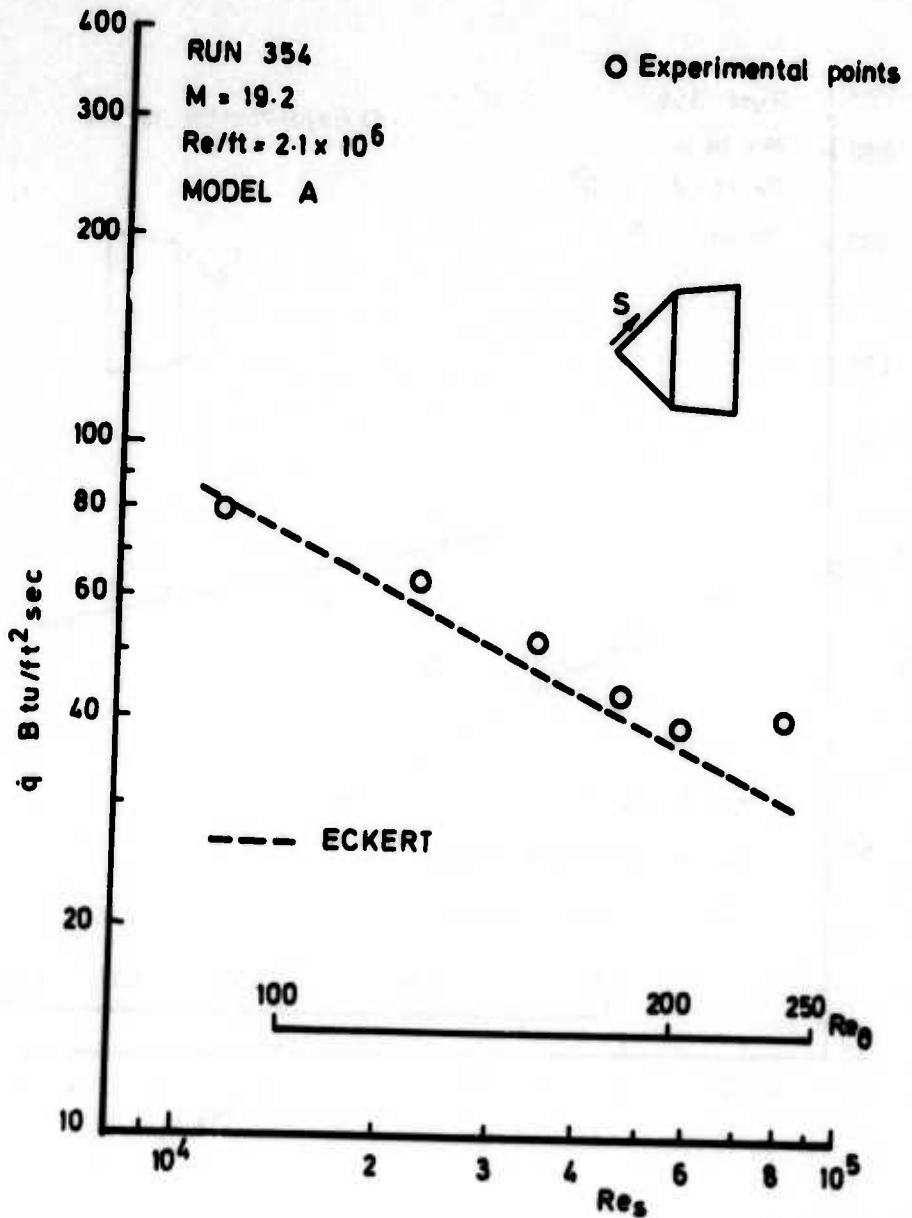


FIG. 10 HEAT TRANSFER DISTRIBUTION ON MODEL A  
 AT  $M = 19.2$   $RE/FT = 2.1 \times 10^6$



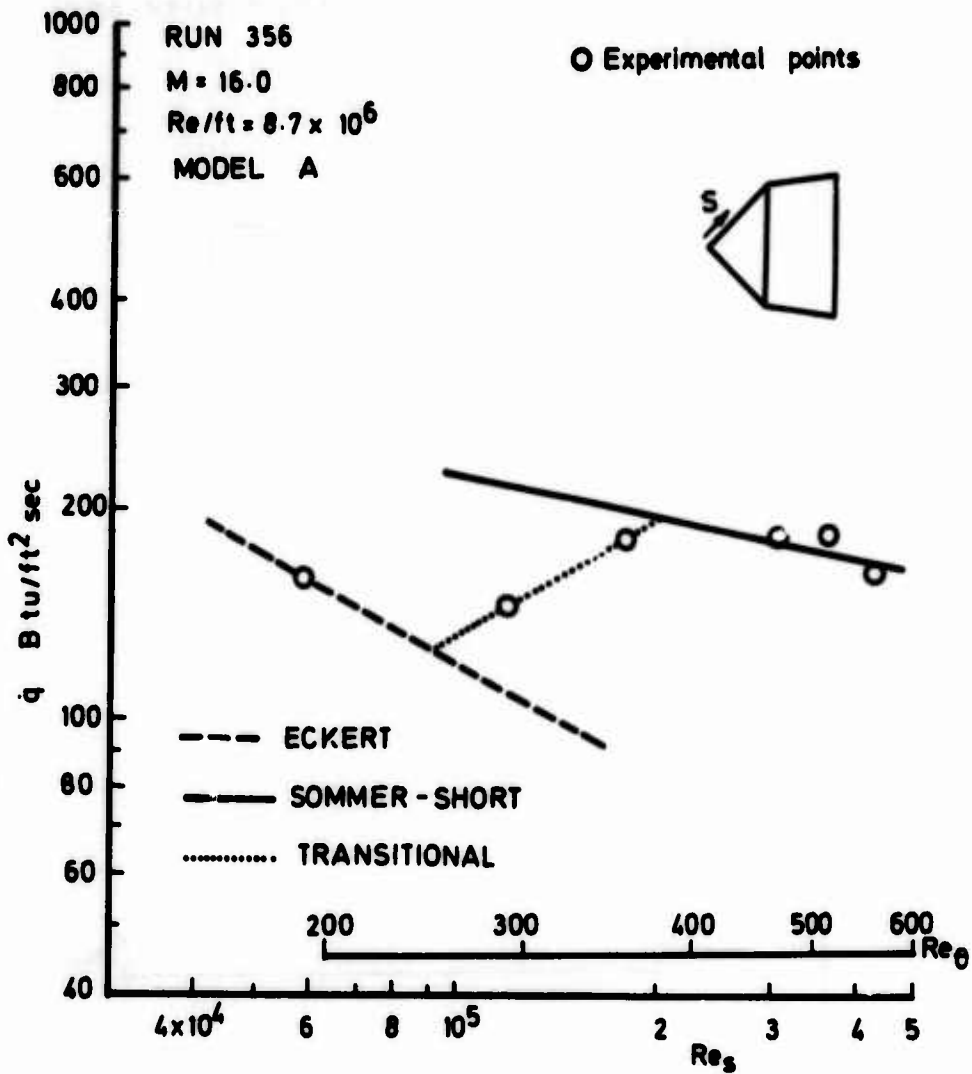


FIG. 11 HEAT TRANSFER DISTRIBUTION ON MODEL A  
AT M = 16.0 RE / FT =  $8.7 \times 10^6$

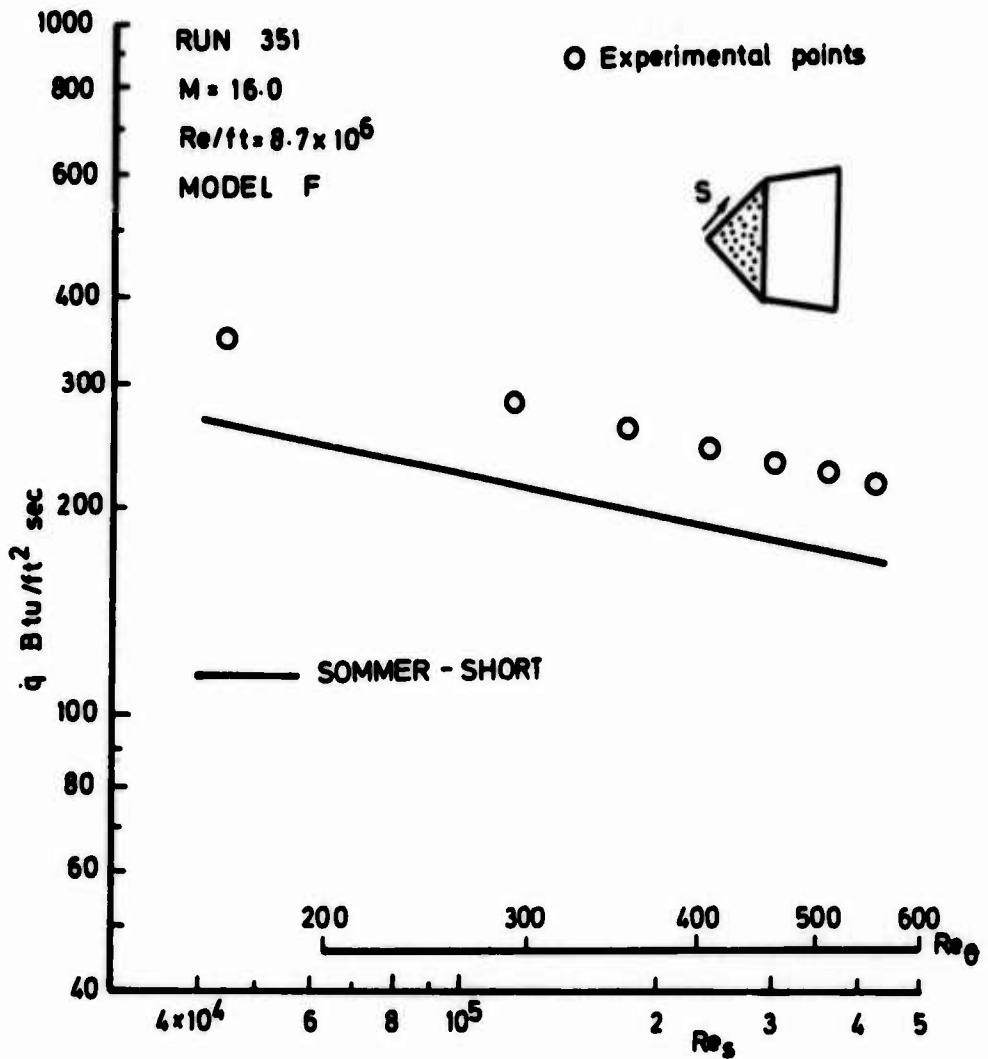


FIG. 12 HEAT TRANSFER DISTRIBUTION ON MODEL F  
AT M = 16.0 RE / FT =  $8.7 \times 10^6$

of the various boundary layer regimes.

In appropriate cases, a straight line is drawn on the data joining the data which appears to be in the laminar and turbulent regimes, in the location thought most appropriate from the position of the experimental points in the plot to describe the transitional heat transfer variation. In most cases the decision is difficult since the density of data points available is very low. It is seen, however, that in most cases the transitional region appears to have a similar, if not larger, extent as the laminar region. This straight line estimate of the heat transfer behaviour in the transition region aids the location of the beginning and end of transition, by the positions at which it bisects the laminar and turbulent data trends.

#### 4. TRANSITION DETECTION RESULTS.

The positions of the beginning and end of transition, using the method described in the last section, from Figs. 5-12 and from analysis of other tests from Refs. 9 and 10 are given in Table 6 to within the resolution of the gauge spacing (i.e. 0.5 in). The positions have been tabulated in order of decreasing Reynolds number and in type of models from rough surfaced to smooth and sharp-nosed to blunt (i.e. models B,F,G,A and C, model B being a model used in the test phase described in Ref. 10 with roughness elements .040 in, as introduced in Section 2.1). This order has been selected to illustrate the trend from configurations with the most likelihood of turbulent flow to those with the most likelihood of laminar flows.

TABLE 6

POSITION OF TRANSITION,  $s_t$ , ON 50° HALF ANGLE BICONIC MODEL FOREBODY.

M	16.2	15.5	19.8	19.3
$Re_s$ at $s = 4$ in	$5.4 \times 10^5$	$3.1 \times 10^5$	$1.3 \times 10^5$	$0.88 \times 10^5$
$Re_\theta$ at $s = 4$ in	600	466	295	249
$Re_k^\dagger$	500	290	120	83
$T_e$ °K	1750	1840	2200	1900
<b>MODEL</b>				
very Rough Model (B)	..... $s_t < 1.5$ in (Run 214)	-	-	$2.0 < s_t < 2.5$ (Run 213)
Rough Sharp (F)	$s_t < 0.5$ (351) $s_t < 0.5$ (352, $\alpha = 10^\circ$ )	-	-	$2.0 < s_t < 4.0$ (371)
Rough Blunt (G)	$0.5 < s_t < 1.0$ (353)	$0.5 < s_t < 1.5$ (376)	-	$2.0 < s_t < 4.0$ (377)
Smooth Sharp (A)	$1.0 < s_t < 1.5$ (356)	$1.5 < s_t < 2.5$ (378)	----- $s_t > 3.5$ [204, $\alpha = 0^\circ$ 206, $\alpha = 10^\circ$ 207, $\alpha = -10^\circ$ 355, $\alpha = 10^\circ$ (cross flow)]	----- $s_t > 3.5$ [354, $\alpha = 0^\circ$ 209, $\alpha = -10^\circ$ 210, $\alpha = +10^\circ$ ]
Smooth Blunt (C)	$1.0 < s_t < 2.0$ (380)	-	----- $s_t > 3.5$ [284, $\alpha = 0^\circ$ 285, $\alpha = +10^\circ$ 286, $\alpha = -10^\circ$ ]	----- $s_t > 3.5$ (287)

..... Turbulent flow over whole model

† For a roughness height of 0.004 in.

----- Laminar flow over whole model

It can be seen from Table 6 that the rough sharp-nosed models appear to have turbulent flow over the whole surface ( or at least over the surface in which heat transfer rates can be measured) for the highest Reynolds numbers. All smooth models for the  $M_{nom} = 20$  cases (i.e. in which the lowest Reynolds numbers are achieved) have entirely laminar flow over them. All other cases have present transitional flow. Summarizing the trends, it is seen that, as expected, surface roughness and increasing unit Reynolds number advances the transition point. Most generally, nose bluntness tends to retard the transition point. One exception to this is at the lowest Reynolds number case when bluntness on the rough surface model advances the transition point (Runs 377 and 379). Although tests were made on models at incidence, it is unfortunate that no information on the behaviour of transition on the windward, leeward or cross-flow surfaces with angle of attack could be discerned since they were all either fully laminar or fully turbulent cases. It is suggested that further tests to examine these trends should be most fruitful.

Because of the sparse amount of data presently available and also the crudeness of the momentum thickness calculation used it was decided to present the transition location results as Reynolds number ranges in which fully laminar or fully turbulent flow was always achieved in all configurations. Figs. 13 and 14 were thus devised to obtain preliminary ranges using the parameters  $Re_{\theta}$  and  $Re_x$ . The influence of the freestream Mach number change in the tests on the flow on the model surface can be considered as affecting only the surface unit Reynolds number and to a small extent surface static temperature. In Figures 13 and 14 curves of  $Re_{\theta}$  (where  $\theta$  is the calculated laminar

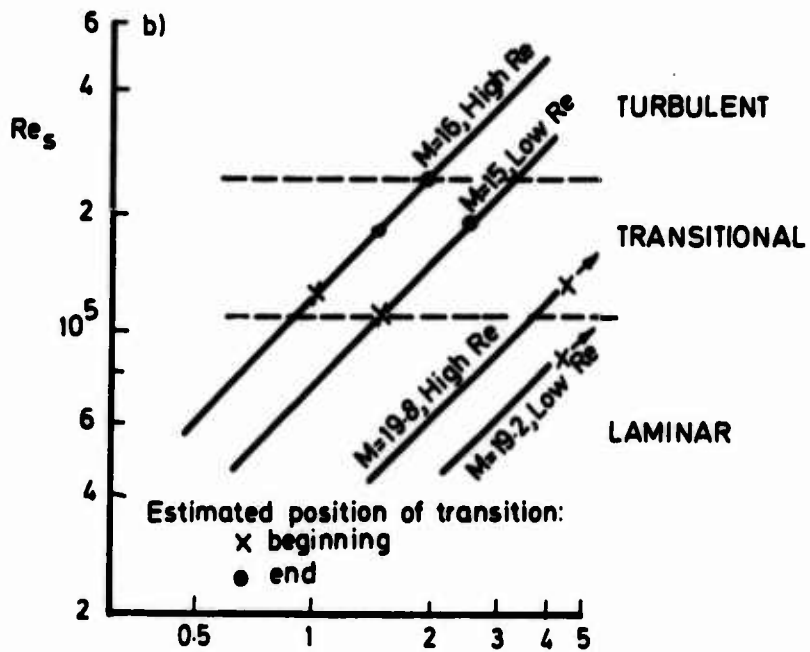
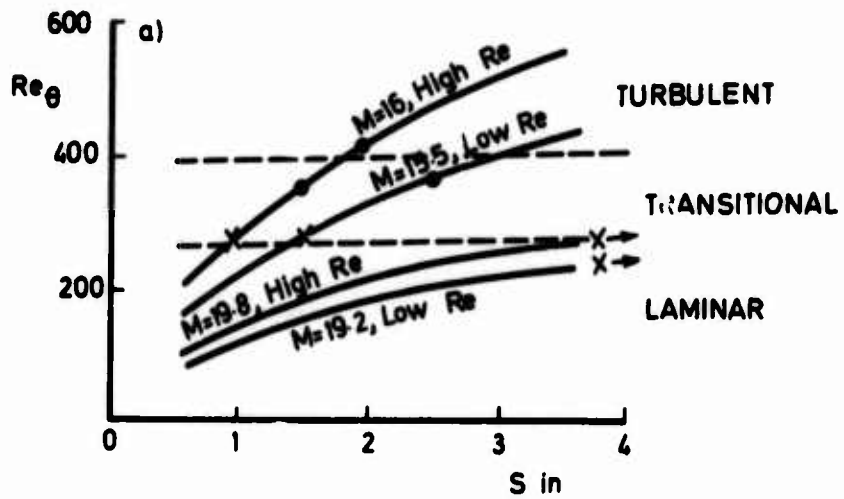


FIG. 13 ESTIMATION OF LOCATION OF BOUNDARY LAYER  
 FLOW REGIMES IN  $Re_\theta$  AND  $Re_s$   
 SMOOTH MODELS

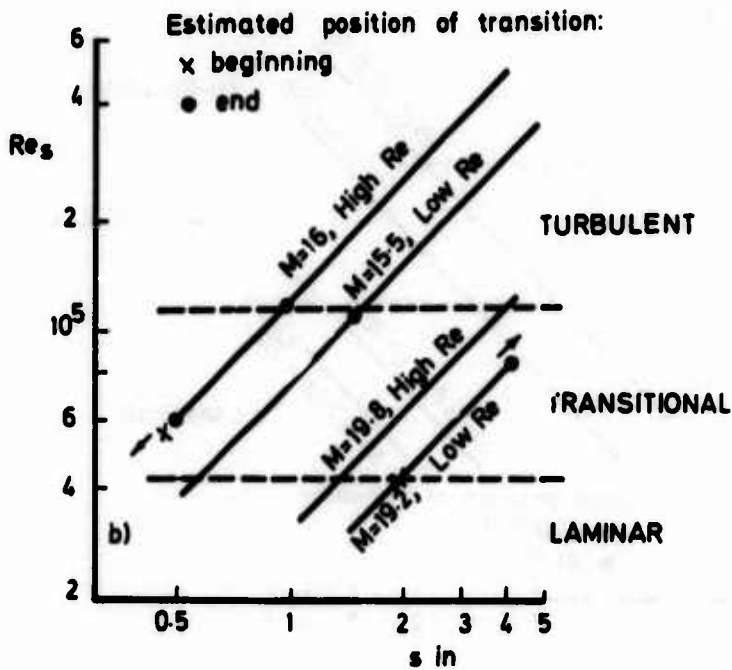
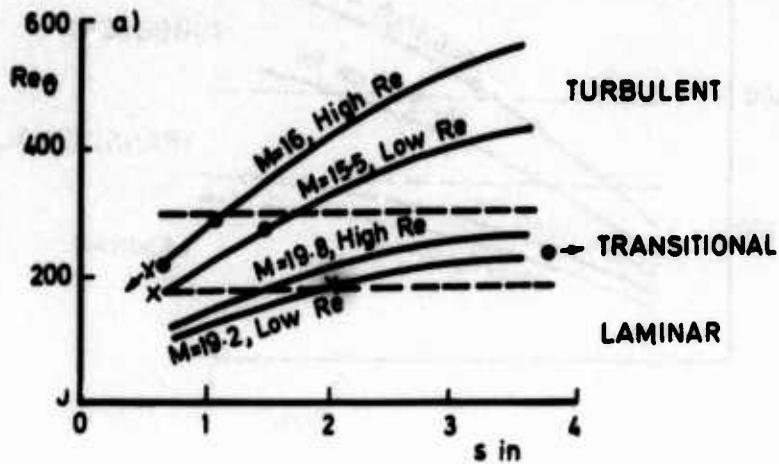


FIG. 14 ESTIMATION OF LOCATION OF BOUNDARY LAYER FLOW REGIMES IN  $Re_\theta$  AND  $Re_s$   
 ROUGH MODELS

value of the momentum thickness on the cone surface) and  $Re_s$  are plotted against distance from the nose of sharp nosed  $50^\circ$  half angle cones placed in each of the four basic Longshot test flows. The transition positions from Table 6 are then plotted on these curves. Such points enable estimates of the Reynolds number ranges of boundary layer flow regimes to be assessed.

The results illustrate that for the smooth surfaced models, laminar flow is found to exist at  $Re_\theta < 270$  and  $Re_s < 10^5$ ; whilst turbulent flow is found to exist at  $Re_\theta > 400$  and  $Re_s > 2.5 \times 10^5$  ( see Figs. 13a and 13b). For the rough surface models laminar flow is found to exist for  $Re_\theta < 170$  and  $Re_s < 4 \times 10^4$  whilst turbulent flow is likely to exist at  $Re_\theta > 300$  and  $Re_s > 10^5$ . ( see Figs. 13b and 14b). The range of Reynolds number based on the roughness height  $k = 0.004$  in. examined was  $83 < Re_k < 500$ .

As is pointed out in the introduction, transition correlations should not be generalised to cover all possible situations, however it is suggested that the above criteria can be applied to cases of flows, simulating those encountered during re-entry, over surfaces at high angles of attack and for the particular surface roughnesses tested. Further tests will enable further correlation parameters, (e.g. nose bluntness, surface roughness, model incidences, unit Reynolds number, etc) to be included.

It is interesting to compare with correlations used by designers of re-entry vehicles. An example, recommended for use for the NASA Space Shuttle by Helms (Ref. 16) is :

$$\frac{(Re_\theta)_t}{Me} = 225$$



Since the surface Mach number on the models in the present tests is approximately 1.4, (with a flow static temperature from 1750°K to 2200°K), then the transition Reynolds number predicted by this correlation is 315. This is seen to show excellent agreement with the test since it has almost exactly mid-way between the limits of transition given by the present smooth model tests.

## SECTION IV

### CONCLUSIONS.

Heat transfer measurements have been used to study the state of the boundary layer on pointed and blunt nosed , smooth and rough surfaced  $50^\circ - 8^\circ$  biconic models at Mach numbers from 15 to 20. The flow on the forebody surface has a Mach number of 1.4 with static temperatures from  $1750^\circ\text{K}$  to  $2200^\circ\text{K}$ . Eckert reference enthalpy theory underestimates laminar data by 10 %. Sommer and Short reference enthalpy theory agrees with smooth wall turbulent data but underestimates the rough wall data by 35 %. The transition region, when present, is often of the same length as the laminar region itself.

For smooth surface models laminar flow was always detected at  $Re_\theta < 270$  and  $Re_s < 10^5$ , whilst turbulent flow was detected at  $Re_\theta > 400$  and  $Re_s > 2.5 \times 10^5$ . For the 0.004 mean element height rough surfaced models laminar flow was detected at  $Re_\theta < 170$  and  $Re_s < 4 \times 10^4$  whilst turbulent flow existed at  $Re_\theta > 300$  and  $Re_s > 10^5$ . The range of Reynolds numbers based on a roughness height,  $k$ , of 0.004 in. examined was  $83 < Re_k < 500$ . The smooth surfaced model data agreed well with a transition criterion used for a similar flow range for application to the Space Shuttle.

Further accumulation of data in future test series could enable a wider range of parameters to be incorporated in the crude correlation presented.

## REFERENCES

1. M.V. MORKOVIN : Critical Evaluation of Transition from Laminar to Turbulent Shear Layers with Emphasis on Hypersonically Travelling Bodies. AFFDL-TR-68-149, March 1969.
2. L.M. MACK : Boundary Layer Stability Theory. Report 900-277, Rev. A, 1969, Jet Propulsion Laboratory, Pasadena, Calif.
3. A.M.O. SMITH and N. GAMBERONI : Transition, Pressure Gradient, and Stability Theory. Report ES 26388, 1956, Douglas Aircraft Co. Inc., El Segundo, California.
4. E.L. KISTLER : Boundary Layer Transition : A Review of Theory, Experiment and Related Phenomena. NASA CR-128540, Feb. 1971.
5. E. RESHOTKO : A Program for Transition Research. AIAA Paper 74-130, AIAA 12th Aerospace Sciences Meeting, Washington D.C., January 1974.
6. J.D. MURPHY, M.W. RUBESIN : Re-evaluation of Heat Transfer Data Obtained in Flight Tests of Heat-sink Shielded Re-entry Vehicles. J. Spacecraft and Rockets, Vol. 3, No. 1, January 1966, pp. 53-60.
7. R. HARTUNIAN, A. RUSSO, P. MARRONE : Boundary Layer Transition and heat Transfer in Shock Tubes. 1959 Heat Transfer and Fluid Mechanics Institute (Stanford Univ. Press, Stanford, California, 1959).
8. B.E. RICHARDS, K.R. ENKENHUS : Hypersonic Testing in the VKI Longshot Free Piston Tunnel. AIAA Journal, Vol. 8, No. 6, June 1970, pp. 1020-1025.
9. B.E. RICHARDS : Hypersonic Heat Transfer Measurements on Re-entry Vehicle Surfaces at High Reynolds Number. VKI TN 91, June 1973. (Also AFML-TR-73-187).
10. B.E. RICHARDS, S. CULOTTA, J. SLECHTEN : Heat Transfer and Pressure Distributions on Re-entry Nose Shapes in the VKI Longshot Hypersonic Tunnel. AFML-TR-71-200, June 1971.
11. E. BACKX : The Total Temperature in the Longshot Wind Tunnel - Its Measurements and Evaluation. VKI TN 98, April 1974.

12. P.F. BRINICH : A Study of Boundary Layer Transition and Surface Temperature Distributions at Mach 3.12. NACA TN 3509, July 1955.
13. L. LEES : Laminar Heat Transfer over Blunt-nosed Bodies at Hypersonic Flight Speeds. Jet Propulsion, April 1956, pp. 259-269.
14. E.R.G. ECKERT : Engineering Relations for Skin Friction and Heat Transfer to Surfaces in High Velocity Flow. Journal of Aerospace Sciences, Vol. 22, p. 585, 1955.
15. S.C. SOMMER, B.J. SHORT : Free Flight Measurements of Turbulent Boundary Layer Skin Friction in the Presence of Severe Aerodynamic Heating at Mach Numbers from 2.8 to 7.0. NACA TN 3391, 1955.
16. V.T. HELMS : Evaluation of Boundary Layer Transition Criteria for Space Shuttle Orbiter Entry. NASA TM X 2507, Feb. 1972.